

Cite this: *Chem. Sci.*, 2024, 15, 5349

All publication charges for this article have been paid for by the Royal Society of Chemistry

# Integrative chemoproteomics reveals anticancer mechanisms of silver(I) targeting the proteasome regulatory complex†

Xiaojian Shao,<sup>ab</sup> Fangrong Xing,<sup>ab</sup> Yiwei Zhang,<sup>ab</sup> Chun-Nam Lok<sup>ab</sup> and Chi-Ming Che<sup>ab\*</sup>

Silver compounds have favorable properties as promising anticancer drug candidates, such as low side effects, anti-inflammatory properties, and high potential to overcome drug resistance. However, the exact mechanism by which Ag(I) confers anticancer activity remains unclear, which hinders further development of anticancer applications of silver compounds. Here, we combine thermal proteome profiling, cysteine profiling, and ubiquitome profiling to study the molecular mechanisms of silver(I) complexes supported by non-toxic thiourea (TU) ligands. Through the formation of AgTU complexes, TU ligands deliver Ag<sup>+</sup> ions to cancer cells and tumour xenografts to elicit inhibitory potency. Our chemical proteomics studies show that AgTU acts on the ubiquitin-proteasome system (UPS) and disrupts protein homeostasis, which has been identified as a main anticancer mechanism. Specifically, Ag<sup>+</sup> ions are released from AgTU in the cellular environment, directly target the 19S proteasome regulatory complex, and may oxidize its cysteine residues, thereby inhibiting proteasomal activity and accumulating ubiquitinated proteins. After AgTU treatment, proteasome subunits are massively ubiquitinated and aberrantly aggregated, leading to impaired protein homeostasis and paraptotic death of cancer cells. This work reveals the unique anticancer mechanism of Ag(I) targeting the 19S proteasome regulatory complex and opens up new avenues for optimizing silver-based anticancer efficacy.

Received 13th September 2023  
Accepted 27th February 2024

DOI: 10.1039/d3sc04834a

rsc.li/chemical-science

## Introduction

Platinum-based chemotherapy drugs represented by cisplatin are widely used in cancer treatment.<sup>1</sup> However, clinically used anticancer platinum chemotherapy drugs have shortcomings such as adverse side effects and drug resistance, which has triggered interest in the development of other metal-based anticancer drugs.<sup>2,3</sup> Compared to platinum compounds, silver complexes have rarely been developed for anticancer therapy but have received widespread attention due to their potent antibacterial and antiviral properties against human infections and their low toxicity to humans.<sup>4–8</sup> Although there are sporadic reports on the anticancer effects of silver complexes, most studies are still in the academic trial stage, and few anticancer silver complexes have been approved to enter clinical trials.<sup>9</sup> Furthermore, the anticancer activity conferred by Ag(I)

complexes remains unclear. Nevertheless, the relatively low toxicity and anti-inflammatory properties of silver complexes in humans make them valuable candidates for developing anticancer therapies.

Previous studies have shown that silver complexes and silver nanoparticles have unique anticancer mechanisms.<sup>10</sup> After entering cancer cells, Ag<sup>+</sup> ions are released from the complex, bind to proteins through coordination or are reduced to Ag<sup>0</sup> and aggregate into nanoparticles.<sup>11,12</sup> Ag<sup>+</sup> ions have been shown to preferentially target the sulfur atoms of cysteine and methionine.<sup>13</sup> Ag<sup>+</sup> ions are isoelectronic with Cu<sup>+</sup> ions and may compete with Cu<sup>+</sup> ions to coordinate with copper transporters and deregulate copper homeostasis.<sup>14</sup> Possible protein targets for Ag<sup>+</sup> ions include cysteine-rich proteins and methionine-containing proteins, such as metallothionein, copper chaperones, high-affinity copper transporter CTR1,  $\alpha$ -synuclein, and prion proteins.<sup>15</sup> Because silver complexes tend to anchor to enzymes, they can denature oncogenic proteins, thereby exerting anticancer activity.<sup>6</sup>

The molecular mechanism of anticancer silver complexes is closely related to their ancillary ligands, which determines their water solubility, lipophilicity, redox ability, and Ag<sup>+</sup> ion release rate, leading to their different anti-tumour activities.<sup>16,17</sup> Ligands with strong  $\sigma$ -donors, such as N-heterocyclic carbenes (NHC), stabilize Ag<sup>+</sup> ions and slow their release under cellular

<sup>a</sup>Department of Chemistry and State Key Laboratory of Synthetic Chemistry, The University of Hong Kong, Pokfulam Road, Hong Kong, P. R. China. E-mail: cmche@hku.hk

<sup>b</sup>Laboratory for Synthetic Chemistry and Chemical Biology Limited, Units 1503-1511, 15/F., Building 17W, Hong Kong Science Park, New Territories, Hong Kong, P. R. China

† Electronic supplementary information (ESI) available: Instrumentation, experimental procedures, synthesis and characterization data, details of biological studies, and supplementary figures. See DOI: <https://doi.org/10.1039/d3sc04834a>



conditions.<sup>18,19</sup> Many ligands of anticancer silver complexes are derived from anti-inflammatory drugs, including aspirin, naproxen, nimesulide, and disulfiram.<sup>20–22</sup> Previously, we reported that AgTU, a silver complex supported by the thiourea (TU) ligand, inhibits the inflammatory TNF- $\alpha$ -stimulated response by targeting cysteine of I $\kappa$ B kinase.<sup>23</sup> This complex has been shown to inhibit cancer cell viability at low micromolar concentrations.<sup>24</sup> However, the molecular mechanism of AgTU's action in cancer cells has not been studied from a systematic perspective.

In this study, we applied chemical proteomics techniques, including thermal proteome profiling (TPP) and activity-based protein profiling (ABPP), combined with ubiquitome analysis

to study protein targets related to the anticancer effects of AgTU. Our results suggest that Ag<sup>+</sup> ions released from AgTU act directly on proteasome regulatory subunits, potentially inducing cysteine oxidation and thereby preventing the proteasome from recruiting ubiquitinated proteins for subsequent degradation. AgTU treatment was found to deregulate the ubiquitin-proteasome system (UPS), increase ubiquitinated proteins, and disrupt protein homeostasis in cancer cells. AgTU treatment also impedes the autophagy process and promotes proteasome ubiquitination and aggregation. Disruption of protein homeostasis ultimately triggers paraptosis-like cancer cell death, suggesting the potential of silver(i) complexes

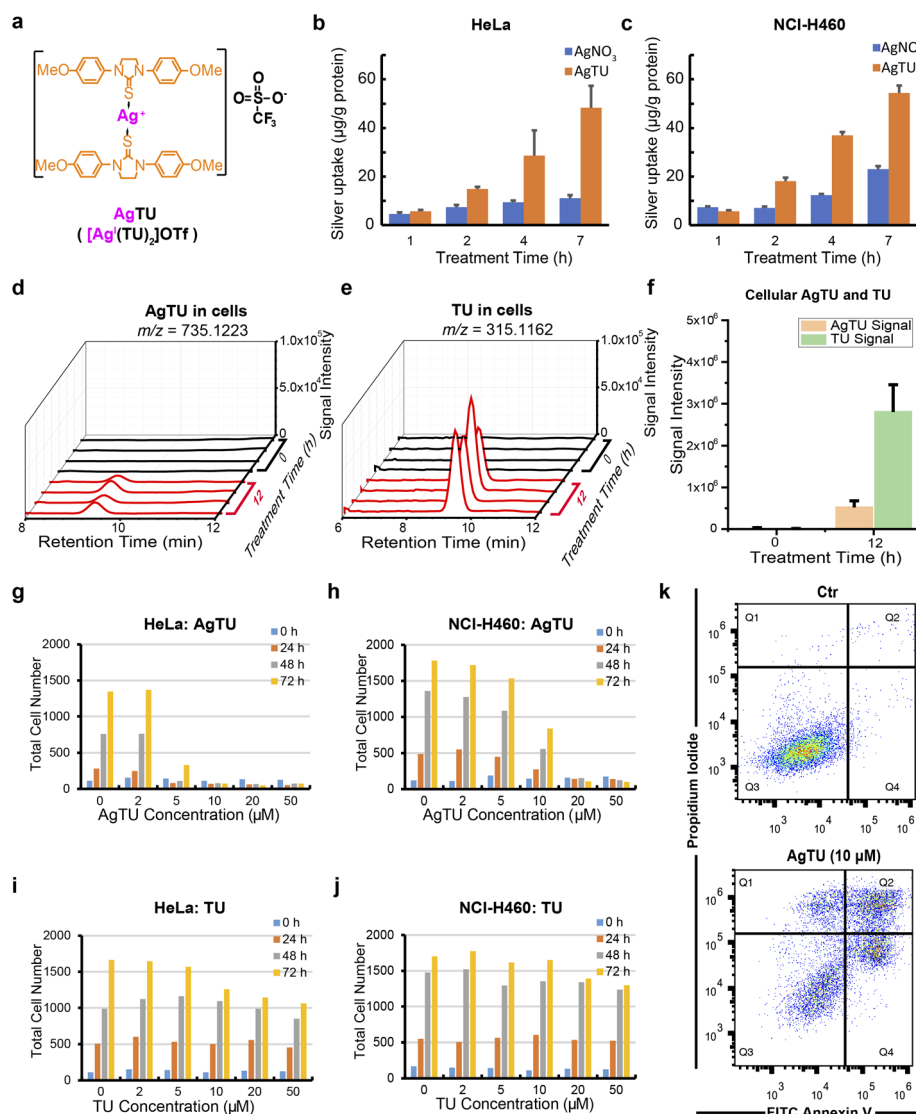


**Fig. 1** MS analysis of cellular uptake of AgTU and its metabolites, and *in vitro* anticancer activity of AgTU. (a) Chemical structure of AgTU ( $[\text{Ag}(\text{TU})_2]\text{OTf}$ ). (b–c) Comparison of cellular uptake of silver using AgTU and  $\text{AgNO}_3$  in (b) HeLa and (c) NCI-H460 cells, where error bars represent standard deviation. (d–f) LC–MS quantification of AgTU ( $m/z = 735.1223$ ) and the release of its TU ligand ( $m/z = 315.1162$ ) in HeLa cells treated with  $10 \mu\text{M}$  AgTU for 0 h and 12 h, respectively: (d) extracted chromatograph of AgTU ( $m/z = 735.1223$ ); (e) extracted chromatograph of TU ( $m/z = 315.1162$ ); (f) comparison of signal intensities of TU and AgTU. Replicate  $n = 4$ . Error bars represent standard deviation. (g–j) High content microscopy analysis of cell viability. HeLa and NCI-H460 cells were treated with a series of concentrations of AgTU or TU for 0–72 h, their total cell numbers were counted: (g) AgTU on HeLa cells, (h) AgTU on NCI-H460 cells, (i) TU on HeLa cells, (j) TU on NCI-H460 cells. (k) Flow cytometry analysis of HeLa cells stained with FITC annexin V and propidium iodide in the control and AgTU groups.



containing non-toxic ligands as effective anticancer therapies by targeting 19S proteasome regulatory particles.

## Results

### AgTU inhibits cancer cell viability *in vitro* and suppresses tumour growth *in vivo*

The synthesis of AgTU and TU ligands has been detailed in our previous paper.<sup>23</sup> Herein, we measured the silver content in AgTU-treated cancer cells using ICP-MS and compared it with AgNO<sub>3</sub>-treated cancer cells (Fig. 1a). The results showed that the silver content in AgTU-treated HeLa and NCI-H460 cells was more than 3 times that of AgNO<sub>3</sub>-treated cells, indicating that TU ligands facilitate the entry of Ag<sup>+</sup> into cancer cells (Fig. 1b and c). The silver content in AgTU-treated HeLa cells gradually increased over time, reaching 5.7 and 48.4 μg per g protein at 1 h and 7 h post-treatment, respectively (Fig. 1b). An ammonium bicarbonate aqueous solution of AgTU (10 mM) was stable for 72 h without any changes observed (Fig. S1a†), while metabolite analysis of AgTU in cells showed a significant increase in the free TU ligand within 12 h (Fig. 1d–f). This suggests that AgTU demetallates and releases Ag<sup>+</sup> ions in the cellular environment. These results also show that TU ligands act as ionophores to facilitate the uptake of AgTU by cancer cells, while Ag<sup>+</sup> ions are the reaction center and are released in the cellular environment.

We studied the anti-proliferative and cytotoxic effects of AgTU on various cancer cell lines using MTT assay (Table 1) and high-content microscopy analysis. AgTU was found to inhibit the viability of a broad spectrum of cancer cell lines with half maximal inhibitory concentration values (IC<sub>50</sub>) ranging from 3.3 to 19.1 μM (Table 1). AgTU exerted antiproliferative effects and cytotoxic effects in HeLa and NCI-H460 cancer cells, as determined by high-content live-dead cell assays (Fig. 1g, h, S1b and c†). In contrast, TU ligand treatment did not have any discernible effect on the viability of a panel of cancer cells (Fig. 1i, j, S1d and e†). These findings show that TU acts as a nontoxic ligand for Ag<sup>+</sup> ions, accelerating silver-mediated anticancer activity. Flow cytometry analysis through annexin V and propidium iodide cell staining revealed AgTU-induced apoptosis in cancer cells (Fig. 1k). By directly observing AgTU-induced cell morphological changes in HeLa cells, we confirmed that AgTU induces cell death with paraptosis-like phenotypes,<sup>25</sup> including the formation of vacuoles in the cytoplasm, disruption of mitochondria and endoplasmic reticulum structures, and deregulation of mitochondrial respiration (Fig. S2†). AgTU treatment inhibited maximal respiratory capacity as shown in oxygen consumption assay but did not affect glycolysis in extracellular acidification assay (Fig. S2c and

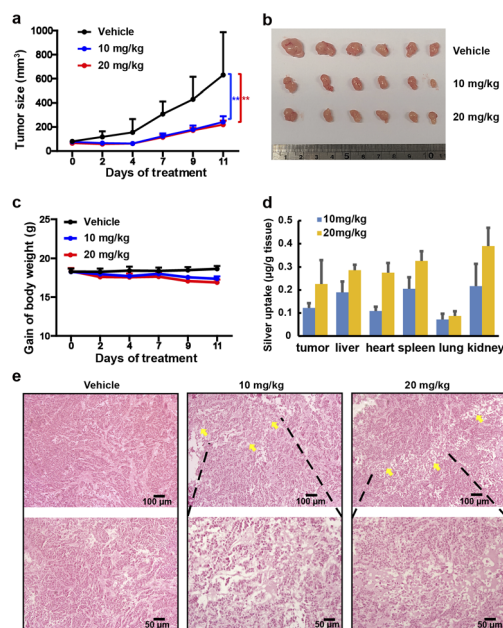


Fig. 2 *In vivo* anti-tumour activities of AgTU. (a) Average tumour volumes of nude mice bearing HeLa tumour xenografts after treatment with vehicle solvent or AgTU at 10 and 20 mg per kg body weight through intraperitoneal injection (\*\**p*-value < 0.01, *n* = 6). (b) Representative photograph of the tumour obtained from nude mice in the solvent control group and AgTU treatment groups. (c) Body weight of nude mice bearing HeLa xenografts. (d) Distribution of silver in tumours and organs extracted from tumour-bearing mice treated with 10 and 20 mg kg<sup>-1</sup> of AgTU, respectively. Error bars represent standard deviation. (e) Representative images of haematoxylin/eosin staining of tumours from vehicle control and AgTU treated groups at the end point (day 11; arrow: necrosis).

d†), revealing that mitochondrial bioenergetics is particularly sensitive to AgTU treatment.

The *in vivo* anti-tumour effects of AgTU were further investigated in nude mice bearing xenografts derived from human HeLa cervical cancer cells. Nude mice were subcutaneously inoculated with HeLa cells and treated with vehicle control, 10, and 20 mg kg<sup>-1</sup> of AgTU, respectively. AgTU treatment every 2–3 days for 11 days inhibited tumour growth, reducing tumour volume by 58.1% and 62.1%, respectively (Fig. 2a and b), and no mouse death or significant body weight loss was observed (Fig. 2c). Determination of the bio-distribution of silver in mice using ICP-MS showed that the accumulation of silver in tumours and organs increased with AgTU concentration (Fig. 2d). At higher doses (20 mg kg<sup>-1</sup>), silver accumulation in tumours was comparable to that in the liver, heart, spleen, and kidneys, and much higher than accumulation in the lungs.

Table 1 *In vitro* cytotoxicity of AgTU on human cancer cell lines (IC<sub>50</sub> (μM), 72 h; mean ± standard deviation)

	HeLa (cervical cancer)	NCI-H460 (lung cancer)	A549 (lung cancer)	HCT-116 (colon cancer)	MDA-MB-231 (breast cancer)	MHCC97L (liver cancer)
AgTU	3.3 ± 0.8	12.2 ± 1.3	19.1 ± 1.3	4.6 ± 0.6	16.1 ± 1.0	6.3 ± 1.5
TU	>100	>100	>100	>100	>100	>100



AgTU treatment resulted in tumour necrosis after 11 days, while no significant toxicity to the liver and kidneys was observed using H&E staining and blood biochemistry assays (Fig. 2e and S3†), showing the efficacy and specificity of AgTU against tumours.

### AgTU targets the 19S proteasome regulatory complex

To reveal the anticancer mechanism of AgTU, we utilized thermal proteome profiling (TPP) to identify its potential protein targets. The premise of this strategy is that binding of a compound to a protein results in a change in the thermal stability of the protein.<sup>26</sup> In HeLa and NCI-H460 cells, the thermal stability of many subunits of the proteasome 19S complex increased after AgTU treatment (Fig. 3a and S4a†). In HeLa cells, gene ontology (GO) enrichment analysis showed that the most enriched protein targets were the proteasome 19S regulatory subunits (Fig. 3b–d), including its base (PSMC1, PSMC2, PSMC4, and PSMC5) and lid (PSMD1, PSMD2, PSMD3, PSMD8, PSMD11, PSMD12, PSMD13, PSMD14, and ADRM1). In

NCI-H460 cells, AgTU treatment resulted in the thermal stabilization of several 19S proteasome subunits, namely, ADRM1, PSMC3, PSMC6, PSMD2, PSMD3, PSMD11, and PSMD13 (Fig. S4b†). The results suggest that AgTU may act on the proteasome regulatory particles, specifically by targeting its ubiquitin receptor (ADRM1) and deubiquitinase (PSMD14). Given that these proteins are involved in recruiting ubiquitinated substrates for deubiquitylation and degradation,<sup>27,28</sup> their targeting implies that AgTU may deregulate the ubiquitin-proteasome system (UPS).

### Cysteines of the 19S proteasome complex are partially oxidized by AgTU

Although AgTU was found to release its TU ligands in the presence of glutathione (GSH) or *N*-acetyl cysteine (NAC), no interaction between the released Ag<sup>+</sup> ions and GSH or NAC was detected in the MS analysis (Fig. 4a and S5†). In-gel fluorescence assays with an iodoacetamide-based fluorescent probe showed reduced cysteine labeling in proteins extracted from the AgTU-

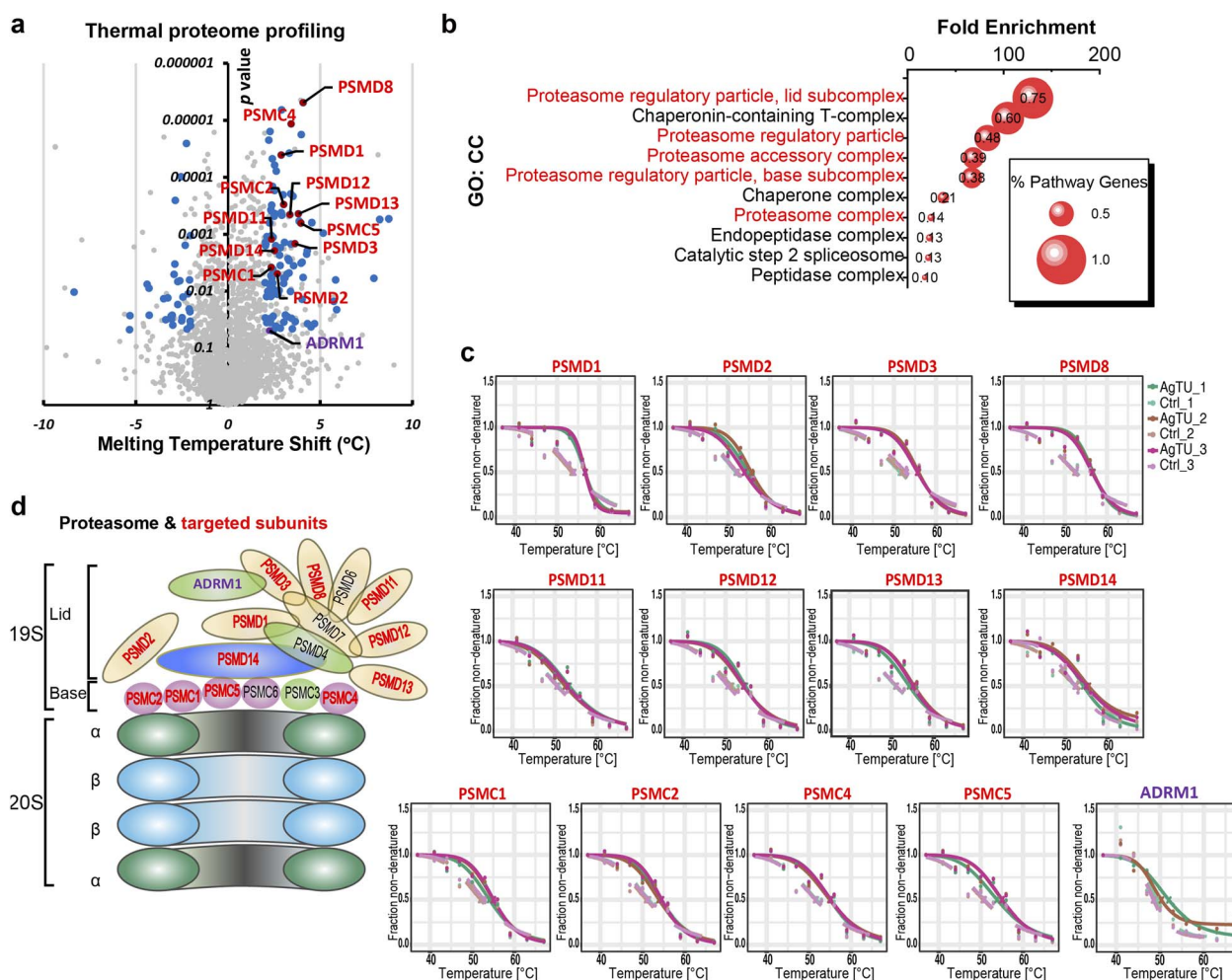
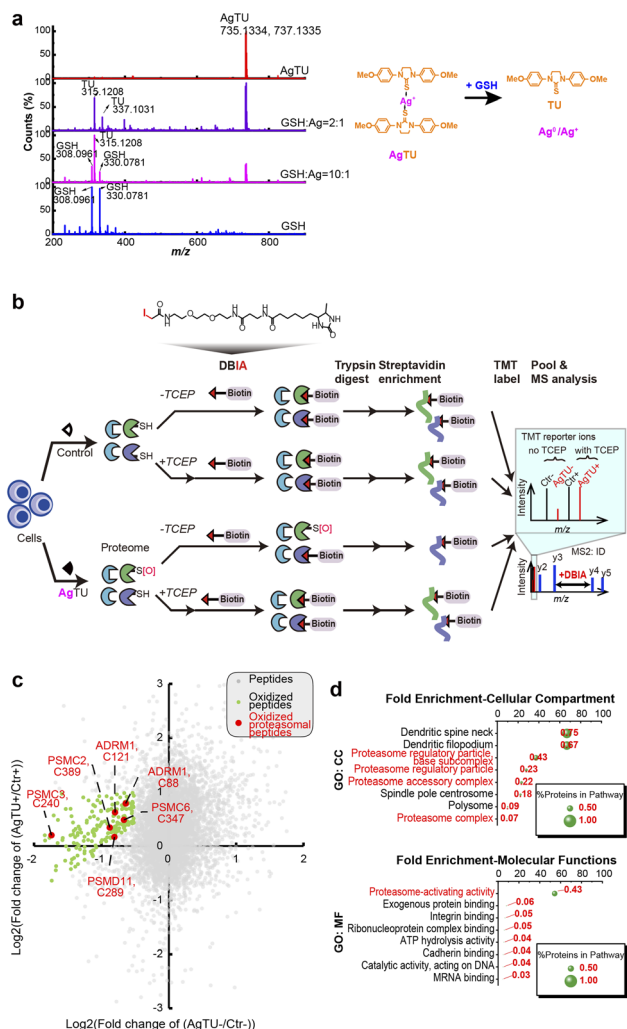


Fig. 3 Target identification using thermal proteome profiling (TPP). (a) Volcano plot showing thermal stability changes following AgTU treatment of HeLa cells, with proteasome proteins highlighted in red. (b) Gene ontology enrichment analysis depicting the cellular component analysis of the altered proteins. (c) Melting curves of thermally stabilized 19S proteasome subunits. (d) The 19S proteasome regulatory complex with its targeted subunits highlighted in red and ADRM1 in purple.





**Fig. 4** Cysteine proteome profiling of AgTU-induced cysteine oxidation in HeLa cells. (a) MS analysis of the reaction between AgTU and glutathione (GSH) and the proposed reaction. (b) Chemical structure of DBIA, a cysteine-reactive probe, and the systematic representation of cysteine profiling. AgTU<sup>-</sup> and Ctr<sup>-</sup>, treatment without TCEP; AgTU<sup>+</sup> and Ctr<sup>+</sup>, treatment with TCEP. (c) Fold change in cysteine labeling is shown by comparing cysteine labeling in AgTU<sup>-</sup> with Ctr<sup>-</sup> (x-axis) and AgTU<sup>+</sup> with Ctr<sup>+</sup> (y-axis). Oxidized peptides and their oxidized cysteine sites are annotated in green, while the oxidized proteasomal peptides are marked in red. (d) Gene ontology enrichment analysis of the oxidized peptides regarding their cellular compartment and molecular function.

treated HeLa cells (Fig. S6†). This may be due to direct targeting of cysteine by AgTU or AgTU-induced cysteine oxidation to form disulfide, sulfenic acid, or sulfinic acid groups.<sup>29</sup> Considering the possibility that AgTU induces cysteine oxidation, we then added the reductant tris(2-carboxyethyl)phosphine (TCEP) to reverse the oxidation.<sup>30</sup> AgTU treatment did not reduce the cysteine labeling in the presence of TCEP (Fig. S6†). These findings suggest that Ag<sup>+</sup> ions released from AgTU may induce protein cysteine oxidation.

We analyzed the AgTU-induced cysteine changes from the perspective of the entire proteome (cysteinome), aiming to provide a broader perspective on Ag<sup>+</sup>-induced protein oxidation

and functional changes. We performed activity-based protein profiling (ABPP) by using the cysteine-targeting probe DBIA (desthiobiotinpolyethylene oxide iodoacetamide) combined with the reducing agent TCEP to identify AgTU-mediated cysteine oxidation (Fig. 4b).<sup>31</sup> Our cysteinome study identified 17 746 peptides, of which 50% (8630 peptides) were grafted with DBIA and TMT. The high proportion of DBIA labeling confirmed the success of cysteine probe ligation, and the identification of over 8000 peptides was comparable to recent cysteine profiling studies.<sup>32,33</sup> We used TMT MS2 ions to quantify the signal intensity of the modified peptides and compared the signal intensities of the control and AgTU groups in the absence and presence of TCEP respectively.

By plotting the fold change of cysteine-containing peptides (Fig. 4c), we identified 190 peptides whose DBIA-tagged cysteine was reduced by more than 30% after AgTU treatment. Addition of TCEP also reversed this change, indicating that the AgTU-induced cysteine changes were possibly attributed to cysteine oxidation. Gene ontology (GO) enrichment analysis showed that the most enriched oxidized proteins were proteasome 19S regulatory subunits, including ADRM1 (C88 and C121), PSMC2 (C389), PSMC3 (C240), PSMC6 (C347), and PSMD11 (C289) (Fig. 4d). We then also performed cysteine profiling by using label-free quantification (Fig. S7†), which suggested that ADRM1 (C80 and C88) and PSMC6 (C347) may be oxidized. Cysteine residue C88 of ADRM1 is located in its ubiquitin receptor domain and is responsible for binding ubiquitinated proteins for subsequent deubiquitination and degradation.<sup>34</sup> Taken together, the cysteine profiling data support the TPP data, showing that AgTU targets the proteasome system and may induce oxidation of cysteine in the 19S proteasome complex.

### AgTU induces ubiquitination and aggregation of proteasomes

Given that AgTU targets the 19S proteasome complex, we then employed immunoprecipitation and proteomic analysis to study its impact on overall global protein ubiquitination. First, total proteins were extracted from the control and AgTU treatment groups and digested into peptides, allowing the identification and quantification of ubiquitinated proteins with lysine (K) residues converted to a K-ε-GG motif (Fig. 5a). Peptides with the K-ε-GG motif were then pulled down using antibodies immobilized on beads and subsequently analyzed by mass spectrometry. Approximately 800 ubiquitinated peptides were identified, of which about 150 peptides were more than 2-fold more ubiquitinated (Fig. 5b).

Heatmap visualization and GO clustering analysis revealed that peptides from proteasomes were highly enriched in cluster 2 (upregulation) and ribosomal proteins were highly enriched in cluster 1 (downregulation) (Fig. 5c and d). Proteasome proteins with upregulated ubiquitination levels include PSMA1 (K208), PSMA7 (K27), PSMC2 (K57), PSMD3 (K76), PSMD14 (K152), and VCP (K112). Given that proteasomes are primarily polyubiquitinated,<sup>35</sup> whereas ribosomes may undergo mono-ubiquitination,<sup>36,37</sup> ubiquitome analysis suggests that AgTU may have an impact on both mono-ubiquitination and



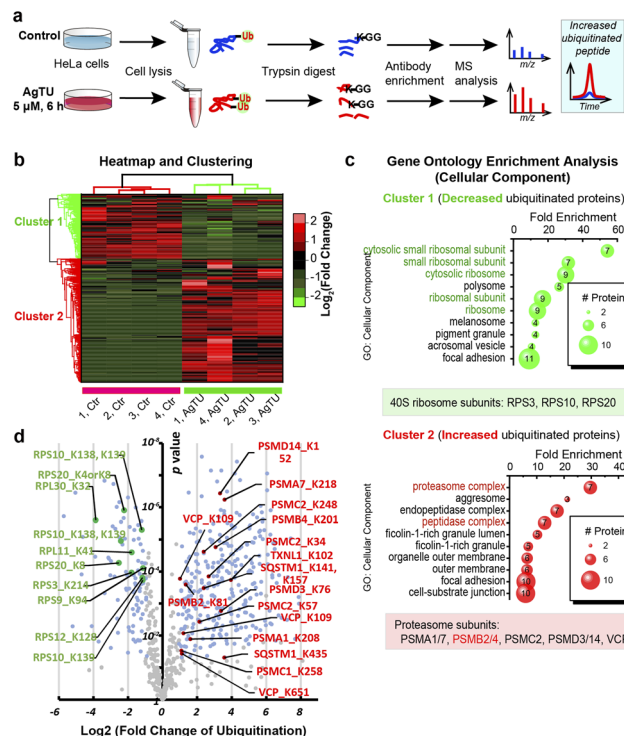


**Fig. 5** Ubiquitome analysis of the AgTU-induced changes in protein ubiquitination. (a) Scheme for ubiquitome analysis in HeLa cells. (b) Heatmap depicting changes in the degree of ubiquitination of peptides. (c) Gene ontology analysis of the proteins with increased and decreased ubiquitination levels. (d) Fold changes of increased ubiquitination of proteasomal subunits and decreased ubiquitination of ribosomal proteins after AgTU treatment.

polyubiquitination levels. The ubiquitome results are consistent with the above TPP and ABPP data, suggesting that AgTU engages and oxidizes the 19S proteasome, alters its stability, and induces accumulation of ubiquitinated proteins, including the accumulation of polyubiquitinated proteasome subunits.

Polyubiquitinated proteins are either directly subject to proteasomal degradation or are degraded by autophagy upon aggregation.<sup>35</sup> We studied AgTU-mediated protein aggregation by analyzing the composition of soluble and insoluble protein fractions (Fig. 6a). Proteomics analysis of the insoluble fractions revealed a general increase in proteasome subunits in AgTU-treated cells, indicating AgTU-induced proteasome aggregation (Fig. 6b). In contrast, there was no significant increase of proteasome subunits in the soluble fraction (Fig. 6b). We observed a significant decrease in the soluble fraction of p62/sequestosome-1 (SQSTM1) and a corresponding increase in the insoluble fraction (Fig. 6c, d, S8a and b†). SQSTM1/p62 is an essential protein that promotes the recruitment of ubiquitinated proteins, and its polymerization is a prerequisite for the recruitment of ubiquitinated protein aggregates and autophagy proteins, such as LC3 to autophagosome.<sup>38,39</sup> The levels of the p62 monomer and aggregates in the soluble and insoluble fractions can be used as an indicator of protein aggregation.<sup>40</sup> After treating HeLa cells with AgTU, we observed a dose- and time-dependent decrease in p62 monomer levels and

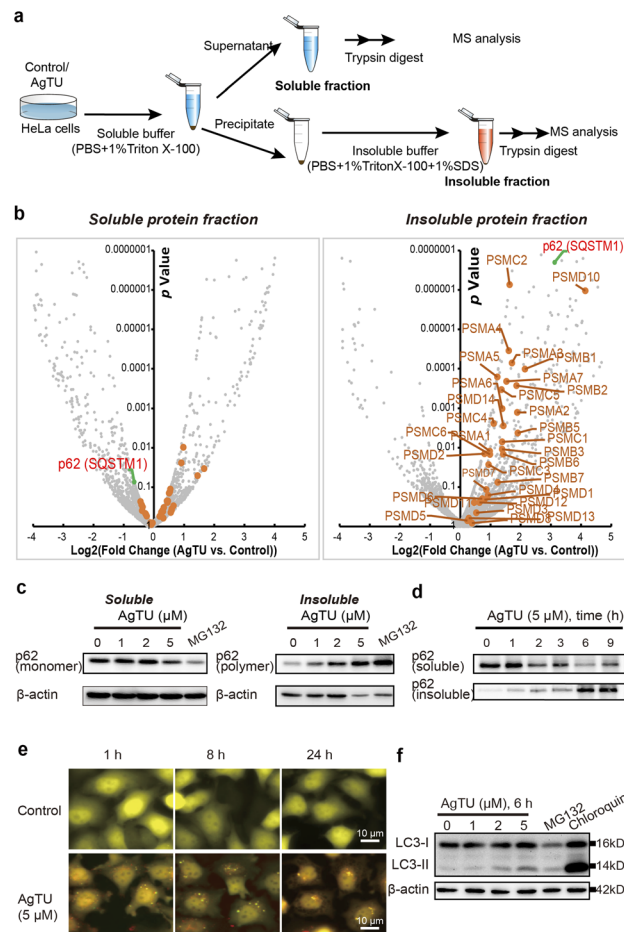


**Fig. 6** AgTU-induced changes in aggregation of proteasome subunits and autophagy in HeLa cells. (a) Schematic representation of the preparation of soluble and insoluble fractions. (b) Volcano plot highlighting fold changes of proteins in soluble and insoluble fractions in AgTU-treated HeLa cells and vehicle control cells, with the proteasomal subunits shown in orange and p62/SQSTM1 in green. (c) Western blot analysis of p62 in soluble and insoluble fractions after 6 h of treatment with AgTU or MG132. (d) Western blot analysis of p62 in soluble and insoluble fractions after treatment with 5 μM AgTU for different times. (e) Monitoring of autophagy changes in tFLC-LC3 HeLa cells. (f) Changes of LC3-I and -II after treatment with AgTU, MG132, or chloroquine (CQ) (as a positive control) for autophagy inhibition.

a corresponding increase in its aggregation degree (Fig. 6c and d). The upregulation of p62 aggregates suggests that AgTU impairs protein homeostasis, leading to accumulation of ubiquitinated proteins and specific dysfunction of the proteasomes and autophagosomes.

Damaged proteasomes have been shown to undergo ubiquitination and autophagic degradation;<sup>41</sup> here we examined the effects of AgTU on autophagy. Using the fluorescent reporter tFLC3 (LC3 tagged with GFP and mRFP in tandem),<sup>42</sup> we observed AgTU-induced accumulation of autophagosomes (yellow puncta) but the presence of a small number of autolysosomes (red puncta) (Fig. 6e). AgTU treatment was also shown to increase LC3-II levels (Fig. 6f and S8c†). The results show that AgTU impairs autophagic flux, which is associated with the



accumulation of damaged proteasomes and ubiquitinated protein aggregates.

### AgTU impairs proteasome activity

Consistent with the results of the proteasome targeting studies mentioned above, AgTU treatment significantly increased the levels of polyubiquitinated proteins in HeLa cancer cells (Fig. 7a and S9a†). Notably, AgTU mainly induces the accumulation of insoluble ubiquitinated proteins, leading to an increase in denatured ubiquitinated protein aggregates and suggesting disruption of protein homeostasis. Our data demonstrate that AgTU targets and inhibits the proteasome, leading to apoptosis- or paraptosis-like cell death, manifested by significant accumulation of cytoplasmic vacuoles, ER morphology changes, and cytoplasmic  $\text{Ca}^{2+}$  release (Fig. S2a and b†). We then pretreated cells with CHX before AgTU treatment, as previous reports showed that CHX can impair paraptosis and sometimes attenuate apoptosis.<sup>43</sup> In addition, CHX has been shown to attenuate cytotoxicity induced by the proteasome inhibitors MG132 and bortezomib.<sup>44,45</sup> Consistent with this, western blot assay showed that CHX impaired AgTU-induced accumulation of polyubiquitinated proteins, possibly due to proteasome inhibition (Fig. 7a). CHX also alleviated AgTU-induced cytotoxicity (Fig. 7b), further demonstrating that AgTU exerts anticancer activities by targeting the proteasome.

AgTU-induced accumulation of ubiquitinated proteins was also demonstrated using HeLa cells containing the Ub<sup>G76V</sup>-YFP protein reporter<sup>46</sup> as a UPS degradation substrate (Fig. 7c).

Accumulation of the UPS reporter protein is triggered by AgTU, albeit to a lesser extent than that by the proteasome inhibitor MG132, which targets the 20S protease activity. Furthermore, we utilized HeLa cells expressing fluorescent GFP-ODC protein<sup>47</sup> as a reporter for ubiquitin-independent proteasome 20S protease activity (Fig. 7d). While MG132 induced significant accumulation of the reporter protein, AgTU did not. We also evaluated the effect of AgTU on cellular 26S and 20S proteasome activity by performing in-gel protease activity assay using the switch-on fluorescent proteasome substrate suc-LLVY-AMC (Fig. 7e and S9b†). The results showed that AgTU down-regulated the 20S and 26S proteasome protease activities, but not to a different extent compared to MG132, which completely inhibited the activity through the target 20S complex (Fig. 7e). The effect of AgTU on 20S proteasome chymotrypsin-like peptidase activity was also examined using a homogeneous fluorometric assay of suc-LLVY-AMC hydrolysis (Fig. S10†). The results showed that AgTU could partially inhibit the proteasome activity, but not to the same extent as MG132, which completely inhibited the protease activity of the 20S proteasome. In summary, our results indicate that consistent with the TPP and cysteine profiling analysis described above, AgTU preferentially targets the 19S proteasome regulatory subunits rather than the 20S proteolytic core.

## Discussion

It has been well documented for decades that silver complexes offer alternative anticancer drug candidates that circumvent

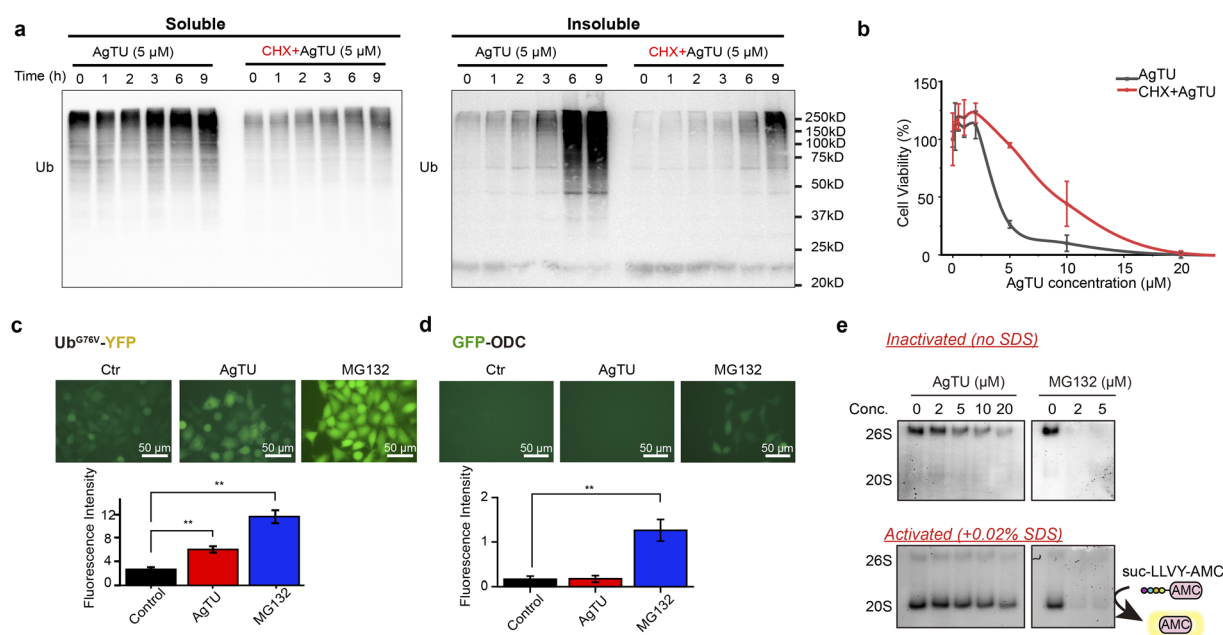


**Fig. 7** Effects of AgTU on proteasomal functions. (a) Ubiquitination changes after treatment of HeLa cells with AgTU for different times in the presence and absence of cycloheximide (CHX), in soluble buffer and insoluble fractions. The protein loading was normalized among samples. (b) Comparison of cell viability after AgTU treatment in the absence and presence of CHX, assessed through MTT assay. \*\* $p < 0.01$ . (c) Monitoring of protein ubiquitination changes using HeLa cells expressing the Ub<sup>G76V</sup>-YFP reporter after treatment with vehicle control, AgTU, or MG132. (d) Monitoring of proteasomal protease activity using HeLa cells containing the fluorescent GFP-ODC reporter. (e) In-gel proteasome activity assay of HeLa cells treated with AgTU, H<sub>2</sub>O<sub>2</sub>, or MG132 in buffers without or with SDS to activate the 20S proteasome. Error bars represent standard deviation.



anticancer drug resistance and are less cytotoxic to humans.<sup>48</sup> However, the anticancer mechanism action of silver complexes needs to be studied from a systematic perspective to facilitate their optimization and development. In this work, we combine several chemoproteomic strategies to identify protein targets of silver complexes to elucidate silver-based anticancer mechanisms.

By developing the silver thiourea complex AgTU and examining its cytotoxicity, our research shows that the coordination of silver ions with nontoxic TU ligands can promote the uptake of silver by cancer cells, making it more effective against cancer than silver nitrate (Fig. 1). The anticancer activity was significantly enhanced. In the cellular environment, AgTU was found to release Ag<sup>+</sup> ions to exert its anticancer effects. AgTU demonstrated potent antiproliferative activity against a panel of cancer cell lines and anti-tumour activity in mice xenograft models (Fig. 2).

To reveal its anticancer mechanism, we combined several chemoproteomics strategies to resolve its protein targets. Thermal proteome profiling revealed that AgTU acts directly on many subunits of the 19S proteasome complex, which has a total of 18 subunits, 13 of which were identified as potential targets in HeLa cells (Fig. 3). The proteasome is a promising anticancer target because it is highly expressed in cancer cells and is responsible for clearing damaged proteins in cells.<sup>49,50</sup> Therefore, proteasome inhibitors are considered to be valuable compounds for the treatment of various cancers.<sup>51,52</sup> Many proteasome inhibitors are in clinical trials for anticancer therapy, and older drugs are being repurposed to evaluate their inhibitory effects against proteasome.<sup>53,54</sup> Several proteasome inhibitors in clinical trials have shown broad anticancer properties and have different primary targets, including the targeting proteasome 20S protease and 19S proteasome-associated deubiquitinases, PSMD14, UCHL5, and USP14, as well as the ubiquitin receptors ADRM1 and PSMD4.<sup>47,55–58</sup> In the proteasome, the 19S complex serves to recognize ubiquitin-tagged substrates, cleave their polyubiquitin chains, unfold the protein, and transfer it to the catalytic 20S in the core.<sup>53</sup> Our study found that AgTU specifically acts on the 19S proteasome regulatory complex, and the components engaged by AgTU include PSMD14, which breaks down polyubiquitin chains, and ADRM1, which recruits ubiquitinated proteins. Directly targeting the 19S proteasome with the silver complex has the potential to be developed as a novel cancer therapy.

Silver(I) ions have a d<sup>10</sup> electronic configuration, are considered “soft” Lewis acids, and exhibit strong reactivity toward cysteine.<sup>59,60</sup> Cysteine residues often appear in the catalytic center of enzymes, affecting their activity and interactions with potential inhibitors.<sup>61–64</sup> In addition, cysteine can be oxidized to form disulfide bonds, sulfenic acid, sulfinic acid, or sulfonic acid, greatly affecting protein structure and function.<sup>65</sup> Previous studies have shown that targeting proteasome subunits can alter the structure and function of proteasome, leading to the accumulation of polyubiquitinated proteins and impairing protein homeostasis.<sup>28</sup> Through cysteine profiling, we found that AgTU treatment induced changes in the oxidation state of the cysteinome sulphur atom. Since thermal proteome

profiling (Fig. 3) and ubiquitome data (Fig. 5) indicate that AgTU targets proteasome regulatory complexes, we performed GO analysis of the cysteine profiling showing that the cysteine oxidized protein profile in AgTU-treated cells was enriched in proteasome proteins (Fig. 4c and d). AgTU may induce cysteine oxidation *in vitro* (Fig. 4a and S5<sup>†</sup>), so we focused on how AgTU treatment affects protein cysteine oxidation in the cysteine profiling analysis, especially on those proteasome subunits that contain reactive cysteines. AgTU targets cysteines of proteasome regulatory subunits, such as the C88 and C121 residues of ADRM1 (Fig. 4), both of which are located in the ubiquitin receptor domain and are responsible for recruiting ubiquitinated proteins for degradation. Previous studies reported that proteasome activity can be regulated through oxidation of proteasome subunits,<sup>66</sup> and therefore oxidation of the ADRM1 cysteine may interfere with the degradation process. However, overall proteasome oxidation levels ranged from 49% to 74%, indicating that AgTU treatment induced mild oxidation. Several other cysteines in the 19S proteasome regulatory complex, including PSMC2 (C389), PSMC3 (C240), PSMC6 (C347), and PSMD11 (C289), are also mildly oxidized. Partial oxidation of cysteines in the 19S complex may deregulate proteasome functions, leading to aggregation of denatured proteins and accumulation of ubiquitinated proteins.

Since AgTU-induced cysteine oxidation of the 19S complex is expected to impair proteasome functions, we performed ubiquitome profiling in AgTU-treated cells. Conjugation of mono-ubiquitin and polyubiquitin to substrate proteins can modulate their subcellular localization, signal regulation, and protein levels and activities through the UPS and autophagy systems.<sup>67</sup> Consistent with its targeting of the 19S proteasome complex, AgTU upregulates the levels of ubiquitinated and aggregated proteins. Further proteomic study of ubiquitinated proteins after AgTU treatment showed increased ubiquitination levels of proteasome subunits (Fig. 5), including 3 subunits from 19S regulatory particles, *i.e.*, PSMC2 (K57), PSMD3 (K51), and PSMD14 (K152), as well as 2 subunits of the 20S core catalytic particle: PSMA1 (K208), and PSMA7 (K27). Furthermore, several reported monoubiquitinated sites of the ribosome, including RPS3 (K214), RPS10 (K138, K139), and RPS20 (K4, K8),<sup>36,37</sup> were observed to be reduced upon AgTU treatment. While AgTU treatment may affect ubiquitinated protein levels, the identity of monoubiquitin *versus* polyubiquitin remains to be determined, as ubiquitinated protein pull-down experiments cannot distinguish the number of protein ubiquitin units.

Proteomics analysis of AgTU-induced protein aggregation confirmed an increase in proteasome aggregates after AgTU treatment (Fig. 6). Ubiquitinated proteasomes are known to be subject to autophagy-mediated degradation.<sup>35</sup> In this work, AgTU impaired the autophagy process, which may be responsible for the accumulation of ubiquitinated proteasomes and their aggregates.

Analysis of proteasome protease activity showed that proteasome activity was deregulated after AgTU treatment (Fig. 7). In western blot analysis, accumulation of ubiquitinated proteins was also observed. Previous studies have shown that metal complexes, including compounds derived from silver,



copper, gold, and rhodium, have the potential to target the proteasome and inhibit proteasome activity.<sup>22,68–70</sup> Specifically, silver ions were found to inhibit the protease activity of the 20S proteasome and the deubiquitinase activity of the 19S proteasome, while the silver diethyldithiocarbamate complex mainly targets the deubiquitinase subunits of the 19S proteasome.<sup>22,71</sup> Our studies demonstrate that AgTU has a distinct mode of targeting proteasome protease activity, leading to possible oxidation of proteasome subunits and an increase in ubiquitinated and aggregated proteasomes in cancer cells. It has been reported that impaired proteasome activity triggers paraptosis which is morphologically characterized by cytoplasmic vacuolation.<sup>72,73</sup> Here, AgTU impairs proteasome activity, which is associated with increased protein aggregates and paraptosis in cancer cells. Proteomic analysis showed that AgTU inhibits proteasome activity by targeting and deregulating the 19S regulatory complex, which is different from the typical proteasome inhibitor MG132 that directly inhibits the proteasome proteolytic center of the 20S catalytic complex.

## Conclusions

In summary, our study demonstrates that AgTU acts on the 19S proteasome complex to impair proteasome protease activity by participating in proteasome cysteine oxidation. Proteasome damage disrupts protein homeostasis in cancer cells, leading to accumulation of misfolded proteins as well as aggregated and ubiquitinated proteins, thereby triggering cancer cell death. Furthermore, our findings demonstrate that AgTU has potent anti-tumour effects in mouse models and cytotoxic effects against a panel of cancer cell lines. This article highlights the importance of integrating multiple chemoproteomics approaches to study the anticancer effects of silver-based compounds and provides a comprehensive strategy to elucidate their anticancer mechanisms.

## Ethical statement

All animal experiments were conducted under the guidelines approved by the Committee on the Use of Live Animals in Teaching and Research of the University of Hong Kong.

## Data availability

All proteome data are uploaded to ProteomeXchange Datasets (PXD042400, PXD043636, PXD048202, PXD042465, PXD042467). Part of experimental supporting data and procedures are available in the ESI and Supporting Data 1.†

## Author contributions

Chi-Ming Che: conceptualization, funding acquisition, investigation, methodology, supervision, writing – review & editing. Xiaojian Shao: conceptualization, data curation, investigation, methodology, software, writing – original draft, writing – review & editing. Fangrong Xing: investigation, methodology. Chun-

Nam Lok: data curation, investigation, writing – review & editing. Yiwei Zhang: data curation, investigation, methodology.

## Conflicts of interest

There are no conflicts to declare.

## Acknowledgements

We acknowledge the funding support from the Laboratory for Synthetic Chemistry and Chemical Biology under the Health@InnoHK Program launched by the Innovation and Technology Commission, The Government of Hong Kong Special Administrative Region of the People's Republic of China, and the financial support from the State Key Laboratory of Synthetic Chemistry. We thank Dr Qian Zhao of The Hong Kong Polytechnic University for initial proteomics analysis. We also thank Dr Kwan Ming Ng for his comment on the mass spectrometry data analysis.

## References

- 1 K. Peng, Y. Zheng, W. Xia and Z. W. Mao, *Chem. Soc. Rev.*, 2023, **52**, 2790–2832.
- 2 L. Messori and A. Merlino, *Coord. Chem. Rev.*, 2016, **315**, 67–89.
- 3 X. Wang, X. Wang, X. Jin, N. Muhammad and Z. Guo, *Chem. Rev.*, 2019, **119**, 1138–1192.
- 4 C. N. Lok, T. Zou, J. J. Zhang, I. W. Lin and C. M. Che, *Adv. Mater.*, 2014, **26**, 5550–5557.
- 5 S. Medici, M. Peana, G. Crisponi, V. M. Nurchi, J. I. Lachowicz, M. Remelli and M. A. Zoroddu, *Coord. Chem. Rev.*, 2016, **327–328**, 349–359.
- 6 S. Medici, M. Peana, V. M. Nurchi and M. A. Zoroddu, *J. Med. Chem.*, 2019, **62**, 5923–5943.
- 7 M. Cao, S. Wang, J. H. Hu, B. H. Lu, Q. Y. Wang and S. Q. Zang, *Adv. Sci.*, 2022, **9**, e2103721.
- 8 D. Panacek, L. Hochvaldova, A. Bakandritsos, T. Malina, M. Langer, J. Belza, J. Martinova, R. Vecerova, P. Lazar, K. Polakova, J. Kolarik, L. Valkova, M. Kolar, M. Otyepka, A. Panacek and R. Zboril, *Adv. Sci.*, 2021, **8**, 2003090.
- 9 Z. Xu, X. Zha, R. Ji, H. Zhao and S. Zhou, *ACS Appl. Mater. Interfaces*, 2023, **15**, 13983–13992.
- 10 L. Qin, P. Wang, Y. Guo, C. Chen and M. Liu, *Adv. Sci.*, 2015, **2**, 1500134.
- 11 S. Tang and J. Zheng, *Adv. Healthcare Mater.*, 2018, **7**, e1701503.
- 12 K. Kluska, J. Adamczyk and A. Krężel, *Coord. Chem. Rev.*, 2018, **367**, 18–64.
- 13 H. Kozłowski, S. Potocki, M. Remelli, M. Rowinska-Zyrek and D. Valensin, *Coord. Chem. Rev.*, 2013, **257**, 2625–2638.
- 14 L. Chen, J. Min and F. Wang, *Signal Transduction Targeted Ther.*, 2022, **7**, 378.
- 15 A. Hecel, P. Kolkowska, K. Krzywoszyńska, A. Szebesczyk, M. Rowinska-Zyrek and H. Kozłowski, *Curr. Med. Chem.*, 2019, **26**, 624–647.
- 16 W. Liu and R. Gust, *Chem. Soc. Rev.*, 2013, **42**, 755–773.



- 17 T. J. Siciliano, M. C. Deblock, K. M. Hindi, S. Durmus, M. J. Panzner, C. A. Tessier and W. J. Youngs, *J. Organomet. Chem.*, 2011, **696**, 1066–1071.
- 18 C. Hemmert, A. Fabie, A. Fabre, F. Benoit-Vical and H. Gornitzka, *Eur. J. Med. Chem.*, 2013, **60**, 64–75.
- 19 K. A. Ali, M. M. Abd-Elzaher and K. Mahmoud, *Int. J. Med. Chem.*, 2013, **2013**, 256836.
- 20 M. Poyraz, C. N. Banti, N. Kourkoumelis, V. Dokorou, M. J. Manos, M. Simčić, S. Golič-Grdadolnik, T. Mavromoustakos, A. D. Giannoulis, I. I. Verginadis, K. Charalabopoulos and S. K. Hadjikakou, *Inorg. Chim. Acta*, 2011, **375**, 114–121.
- 21 C. N. Banti, A. D. Giannoulis, N. Kourkoumelis, A. M. Owczarzak, M. Poyraz, M. Kubicki, K. Charalabopoulos and S. K. Hadjikakou, *Metallomics*, 2012, **4**, 545–560.
- 22 X. Chen, Q. Yang, J. Chen, P. Zhang, Q. Huang, X. Zhang, L. Yang, D. Xu, C. Zhao, X. Wang and J. Liu, *Cell. Physiol. Biochem.*, 2018, **49**, 780–797.
- 23 I. W. Lin, C. N. Lok, K. Yan and C. M. Che, *Chem. Commun.*, 2013, **49**, 3297–3299.
- 24 K. Yan, C. N. Lok, K. Bierla and C. M. Che, *Chem. Commun.*, 2010, **46**, 7691–7693.
- 25 F. Fontana, M. Raimondi, M. Marzagalli, A. Di Domizio and P. Limonta, *Biochim. Biophys. Acta, Rev. Cancer*, 2020, **1873**, 188338.
- 26 H. Franken, T. Mathieson, D. Childs, G. M. Sweetman, T. Werner, I. Togel, C. Doce, S. Gade, M. Bantscheff, G. Drewes, F. B. Reinhard, W. Huber and M. M. Savitski, *Nat. Protoc.*, 2015, **10**, 1567–1593.
- 27 C. W. Liu and A. D. Jacobson, *Trends Biochem. Sci.*, 2013, **38**, 103–110.
- 28 D. J. Trader, S. Simanski and T. Kodadek, *J. Am. Chem. Soc.*, 2015, **137**, 6312–6319.
- 29 A. A. Saei, H. Gullberg, P. Sabatier, C. M. Beusch, K. Johansson, B. Lundgren, P. I. Arvidsson, E. S. J. Arner and R. A. Zubarev, *Redox Biol.*, 2020, **32**, 101491.
- 30 E. A. Kisty, J. A. Falco and E. Weerapana, *Cell Chem. Biol.*, 2023, **30**, 321–336.
- 31 E. K. Kemper, Y. Zhang, M. M. Dix and B. F. Cravatt, *Nat. Methods*, 2022, **19**, 341–352.
- 32 M. Kuljanin, D. C. Mitchell, D. K. Schweppe, A. S. Gikandi, D. P. Nusinow, N. J. Bulloch, E. V. Vinogradova, D. L. Wilson, E. T. Kool, J. D. Mancias, B. F. Cravatt and S. P. Gygi, *Nat. Biotechnol.*, 2021, **39**, 630–641.
- 33 F. Yang, G. Jia, J. Guo, Y. Liu and C. Wang, *J. Am. Chem. Soc.*, 2022, **144**, 901–911.
- 34 P. Dickson, D. Abegg, E. Vinogradova, J. Takaya, H. An, S. Simanski, B. F. Cravatt, A. Adibekian and T. Kodadek, *Cell Chem. Biol.*, 2020, **27**, 1371–1382.
- 35 W. Li, P. He, Y. Huang, Y. F. Li, J. Lu, M. Li, H. Kurihara, Z. Luo, T. Meng, M. Onishi, C. Ma, L. Jiang, Y. Hu, Q. Gong, D. Zhu, Y. Xu, R. Liu, L. Liu, C. Yi, Y. Zhu, N. Ma, K. Okamoto, Z. Xie, J. Liu, R. R. He and D. Feng, *Theranostics*, 2021, **11**, 222–256.
- 36 A. Garzia, S. M. Jafarnejad, C. Meyer, C. Chapat, T. Gogakos, P. Morozov, M. Amiri, M. Shapiro, H. Molina, T. Tuschl and N. Sonenberg, *Nat. Commun.*, 2017, **8**, 16056.
- 37 A. Garzia, C. Meyer and T. Tuschl, *Cell Rep.*, 2021, **36**, 109468.
- 38 B. Carroll, E. G. Otten, D. Manni, R. Stefanatos, F. M. Menzies, G. R. Smith, D. Jurk, N. Kenneth, S. Wilkinson, J. F. Passos, J. Attems, E. A. Veal, E. Teysou, D. Seilhean, S. Millecamps, E. L. Eskelinen, A. K. Bronowska, D. C. Rubinsztein, A. Sanz and V. I. Korolchuk, *Nat. Commun.*, 2018, **9**, 256.
- 39 Y. Zhang, S. R. Mun, J. F. Linares, J. Ahn, C. G. Towers, C. H. Ji, B. E. Fitzwalter, M. R. Holden, W. Mi, X. Shi, J. Moscat, A. Thorburn, M. T. Diaz-Meco, Y. T. Kwon and T. G. Kutateladze, *Nat. Commun.*, 2018, **9**, 4373.
- 40 D. Sun, R. Wu, J. Zheng, P. Li and L. Yu, *Cell Res.*, 2018, **28**, 405–415.
- 41 D. Hoeller and I. Dikic, *Proc. Natl. Acad. Sci. U.S.A.*, 2016, **113**, 13266–13268.
- 42 S. Kimura, T. Noda and T. Yoshimori, *Autophagy*, 2007, **3**, 452–460.
- 43 D. Nedungadi, A. Binoy, N. Pandurangan, B. G. Nair and N. Mishra, *Cell Biol. Int.*, 2021, **45**, 164–176.
- 44 J. Lavie, H. De Belvalet, S. Sonon, A. M. Ion, E. Dumon, S. Melser, D. Lacombe, J. W. Dupuy, C. Lalou and G. Benard, *Cell Rep.*, 2018, **23**, 2852–2863.
- 45 S. T. Nawrocki, J. S. Carew, K. Dunner Jr, L. H. Boise, P. J. Chiao, P. Huang, J. L. Abbruzzese and D. J. McConkey, *Cancer Res.*, 2005, **65**, 11510–11519.
- 46 V. Menendez-Benito, L. G. Verhoef, M. G. Masucci and N. P. Dantuma, *Hum. Mol. Genet.*, 2005, **14**, 2787–2799.
- 47 B. H. Lee, M. J. Lee, S. Park, D. C. Oh, S. Elsassser, P. C. Chen, C. Gartner, N. Dimova, J. Hanna, S. P. Gygi, S. M. Wilson, R. W. King and D. Finley, *Nature*, 2010, **467**, 179–184.
- 48 Y. H. Lim, K. M. Tiemann, G. S. Heo, P. O. Wagers, Y. H. Rezenom, S. Y. Zhang, F. W. Zhang, W. J. Youngs, D. A. Hunstad and K. L. Wooley, *ACS Nano*, 2015, **9**, 1995–2008.
- 49 H. H. Huang, I. D. Ferguson, A. M. Thornton, P. Bastola, C. Lam, Y. T. Lin, P. Choudhry, M. C. Mariano, M. D. Marcoulis, C. F. Teo, J. Malato, P. J. Phojanakong, T. G. Martin 3rd, J. L. Wolf, S. W. Wong, N. Shah, B. Hann, A. N. Brooks and A. P. Wiita, *Nat. Commun.*, 2020, **11**, 1931.
- 50 X. Lu, U. Nowicka, V. Sridharan, F. Liu, L. Randles, D. Hymel, M. Dyba, S. G. Tarasov, N. I. Tarasova, X. Z. Zhao, J. Hamazaki, S. Murata, T. R. Burke Jr and K. J. Walters, *Nat. Commun.*, 2017, **8**, 15540.
- 51 R. K. Anchoori, B. Karanam, S. Peng, J. W. Wang, R. Jiang, T. Tanno, R. Z. Orłowski, W. Matsui, M. Zhao, M. A. Rudek, C. F. Hung, X. Chen, K. J. Walters and R. B. Roden, *Cancer Cell*, 2013, **24**, 791–805.
- 52 A. L. Goldberg, *J. Cell Biol.*, 2012, **199**, 583–588.
- 53 J. E. Park, Z. Miller, Y. Jun, W. Lee and K. B. Kim, *Transl. Res.*, 2018, **198**, 1–16.
- 54 H. Yang, X. Chen, K. Li, H. Cheaito, Q. Yang, G. Wu, J. Liu and Q. P. Dou, *Semin. Cancer Biol.*, 2021, **68**, 105–122.
- 55 Q. P. Dou and J. A. Zonder, *Curr. Cancer Drug Targets*, 2014, **14**, 517–536.



- 56 Y. Song, T. Du, A. Ray, K. Chauhan, M. Samur, N. Munshi, D. Chauhan and K. C. Anderson, *Blood Cancer J.*, 2021, **11**, 13.
- 57 T. Du, Y. Song, A. Ray, X. Wan, Y. Yao, M. K. Samur, C. Shen, J. Penailillo, T. Sewastianik, Y. T. Tai, M. Fulcinitti, N. C. Munshi, H. Wu, R. D. Carrasco, D. Chauhan and K. C. Anderson, *Blood*, 2023, **141**, 2599–2614.
- 58 J. A. Harrigan, X. Jacq, N. M. Martin and S. P. Jackson, *Nat. Rev. Drug Discovery*, 2018, **17**, 57–78.
- 59 C. Gabbiani, F. Scaletti, L. Massai, E. Michelucci, M. A. Cinellu and L. Messori, *Chem. Commun.*, 2012, **48**, 11623–11625.
- 60 L. V. Puchkova, M. Broggini, E. V. Polishchuk, E. Y. Ilyechova and R. S. Polishchuk, *Nutrients*, 2019, **11**, 1364.
- 61 M. Marzi, M. K. Vakil, M. Bahmanyar and E. Zarenezhad, *BioMed Res. Int.*, 2022, **2022**, 7341493.
- 62 K. Senkane, E. V. Vinogradova, R. M. Suciui, V. M. Crowley, B. W. Zaro, J. M. Bradshaw, K. A. Brameld and B. F. Cravatt, *Angew. Chem., Int. Ed.*, 2019, **58**, 11385–11389.
- 63 X. Shao, F. Ji, Y. Wang, L. Zhu, Z. Zhang, X. Du, A. C. K. Chung, Y. Hong, Q. Zhao and Z. Cai, *Anal. Chem.*, 2018, **90**, 11092–11098.
- 64 C. M. Forester, Q. Zhao, N. J. Phillips, A. Urisman, R. J. Chalkley, J. A. Osés-Prieto, L. Zhang, D. Ruggero and A. L. Burlingame, *Proc. Natl. Acad. Sci. U.S.A.*, 2018, **115**, 2353–2358.
- 65 M. C. Montasell, P. Monge, S. Carmali, L. M. D. Loiola, D. G. Andersen, K. B. Lovschall, A. B. Sogaard, M. M. Kristensen, J. M. Putz and A. N. Zelikin, *Nat. Commun.*, 2022, **13**, 4861.
- 66 M. Qiu, J. Chen, X. Li and J. Zhuang, *Int. J. Mol. Sci.*, 2022, **23**, 12197.
- 67 Z. A. Ronai, *Proc. Natl. Acad. Sci. U.S.A.*, 2016, **113**, 8894–8896.
- 68 Z. Skrott, M. Mistrik, K. K. Andersen, S. Friis, D. Majera, J. Gursky, T. Ozdian, J. Bartkova, Z. Turi, P. Moudry, M. Kraus, M. Michalova, J. Vaclavkova, P. Dzubak, I. Vrobel, P. Pouckova, J. Sedlacek, A. Miklovicova, A. Kutt, J. Li, J. Mattova, C. Driessen, Q. P. Dou, J. Olsen, M. Hajduch, B. Cvek, R. J. Deshaies and J. Bartek, *Nature*, 2017, **552**, 194–199.
- 69 F.-M. Siu, I. W.-S. Lin, K. Yan, C.-N. Lok, K.-H. Low, T. Y.-C. Leung, T.-L. Lam and C.-M. Che, *Chem. Sci.*, 2012, **3**, 1785–1793.
- 70 N. N. Liu, X. F. Li, H. B. Huang, C. Zhao, S. Y. Liao, C. S. Yang, S. T. Liu, W. B. Song, X. Y. Lu, X. Y. Lan, X. Chen, S. G. Yi, L. Xu, L. L. Jiang, C. G. Zhao, X. X. Dong, P. Zhou, S. J. Li, S. Q. Wang, X. P. Shi, P. Q. Dou, X. J. Wang and J. B. Liu, *Oncotarget*, 2014, **5**, 5453–5471.
- 71 A. Filippi, M. Zancani, E. Petrusa and E. Braidot, *J. Plant Physiol.*, 2019, **233**, 42–51.
- 72 D. Lee, I. Y. Kim, S. Saha and K. S. Choi, *Pharmacol. Ther.*, 2016, **162**, 120–133.
- 73 H. J. Lee, D. M. Lee, M. J. Seo, H. C. Kang, S. K. Kwon and K. S. Choi, *Int. J. Mol. Sci.*, 2022, **23**, 2648.

